Electronic and geometric structure of C_{60} on Al(111) and Al(110)

A. J. Maxwell,* P. A. Brühwiler,† D. Arvanitis, and J. Hasselström
Department of Physics, Uppsala University, Box 530, S-751 21 Uppsala, Sweden

M. K.-J. Johansson
Department of Synchrotron Radiation Research, Lund University, Sölvegatan 14, S-223 62 Lund, Sweden

N. Mårtensson
Department of Physics, Uppsala University, Box 530, S-751 21 Uppsala, Sweden

(Received 10 October 1997)

Two new ordered monolayer phases of C_{60} on Al surfaces have been studied using electron spectroscopies and low-energy electron diffraction (LEED). On Al(111), in addition to the previously reported (6×6) phase formed by evaporating with $T_{sample}=620$ K, a metastable $(2\sqrt{3}\times 2\sqrt{3})R30°$ phase can be produced with $T_{sample}=300$ K. This phase exhibits the first LEED pattern reported for an unannealed C_{60} overlayer. On Al(110), when evaporations are also made with $T_{sample}=620$ K, LEED shows the presence of a monolayer with a pseudo-$c(4\times 4)$ structure. Al $2p$ photoemission for C_{60}/Al(110) and for $(2\sqrt{3}\times 2\sqrt{3})R30°$ C_{60}/Al(111) reveals no evidence of strong substrate reconstruction. The perturbation of the geometric and electronic structure of the C_{60} molecule due to the bonding interaction with the Al surface increases in the order C_{60}/Al(110), $(2\sqrt{3}\times 2\sqrt{3})R30°$ C_{60}/Al(111), (6×6) C_{60}/Al(111), as demonstrated using element-specific probing of the valence band with x-ray absorption and C $1s$ shakeup. The bond has covalent character in all three cases. Symmetry-induced splitting in the $5h_u$-derived level is observed using valence photoemission, and is particularly clear for C_{60}/Al(110). The stability of the equilibrium structures can be qualitatively understood from considerations of the energetics of the overlayer compression and the chemical bond between adsorbate and substrate. Work-function measurements for these and other C_{60} overlayer systems cannot, in general, be understood within a simple description involving the addition of a dipole to the surface potential. [S0163-1829(98)00412-3]

I. INTRODUCTION

The bonding of C_{60} to other materials strongly influences many interesting properties, such as superconductivity and the rich endohedral and exohedral chemistry. One approach to understanding the bonding characteristics of C_{60} is to study the interaction between this fullerene and surfaces of other materials. For thin films of C_{60}, chemical bonding effects due to substrate-adsorbate interactions appear only to be important for the molecules in direct contact with the surface,[1–4] and a great deal of effort has been invested in understanding the electronic and geometric structure of such monolayer systems. In order to describe previous work and illustrate the way in which the present study is related to it, we present in Table I a summary of results for C_{60} monolayers on a number of substrates. The table shows the evolution of the bonding characteristics, as well as the observed geometric structures, as the substrate-adsorbate bond strength increases. We use the desorption temperature as a measure of this strength.

On inert surfaces such as GeS(001),[5] graphite,[6,7] and[8] SiO_2 [row (a) in Table I], the desorption temperatures for submonolayers of C_{60} are all close to that at which solid fullerite begins to sublime rapidly,[9] i.e., $450-500$ K. The strength of the substrate-adsorbate interaction is, therefore, similar to that of the interfullerene bonding in solid C_{60}, implying that it is essentially van der Waals in nature. The relative strengths of the C_{60} substrate and C_{60}-C_{60} bonds influence the structure of the overlayers formed on each substrate. On these surfaces, the fullerenes form hexagonal overlayers with nearest neighbor distances (NND's) very close to the value of 10.04 Å reported for solid C_{60}.[10,6] This suggests that the adsorbate-adsorbate interaction is the most important factor in determining the geometry adopted. It is only on GeS(001) that, as a result of the favorable lattice matching, commensurate overlayers are able to grow.[10–13] In row (c) of Table I is a bonding category containing Au, Ag, and Cu substrates, and C_{60} monolayers on low-index faces of these metals have been extensively studied. The substrate-adsorbate bond for these systems is found to be significantly stronger than for the surfaces discussed above, with desorption temperatures for the first layer close to 800 K.[14,15] Common for these substrates is a strong ionic component to the bonding, with charge transferred from the metal to the fullerene $5t_{1u}$-derived lowest unoccupied molecular orbital (LUMO). Shifts of the totally symmetric ''pentagonal pinch'' vibrational mode give a measure of the partial filling of this state.[16,17] Charge from the substrate has also been observed directly in the LUMO of C_{60} using photoemission (PES) on Au(110),[18] Ag(111),[19] Cu(111),[20] and polycrystalline Ag and Cu.[21] The effect of the partial occupation of the LUMO in the unoccupied valence band has also been observed as a decrease in intensity of the resonance derived from this level in C $1s$ x-ray absorption spectroscopy (XAS), for C_{60} on[22] Cu(001) and[20] Cu(111), as well as inverse photoemission on Cu(111).[23]

TABLE I. A summary of previous and present results for C_{60} monolayer systems. The equilibrium bond lengths given are for the lowest-energy structure, at the reported coverage, which is closest to a monolayer. The desorption temperature represents the temperature for which the entire first layer is desorbed in an ill-defined ''short'' period. Where a reference is indicated with the substrate it refers to all the data given in the table for that surface. Substrates for which insufficient data are available are omitted. An illustration of the special nature of the C_{60}-Al bond discussed in the text is given by the similarity between the characteristics of columns 1 and 4 in rows (b) and (d), in contrast to the the correlation between columns 2 and 3 in rows (b) and (c).

	Substrate	1 Type of bonding	2 Approximate desorption temperature (K)	3 Mobility at room temperature	4 Equilibrium C_{60}-C_{60} bond lengths (Å)
(a)	Graphite	weak,	500[a]	mobile[b]	10.01[c]
	GeS(001)[d]	predominantly	490	mobile	10.02
	SiO_2[e]	van der Waals	470	mobile	
(b)	Al(110)[f]	intermediate,	730		9.91, 11.44, 12.13
	Al(111)[g]	predominantly covalent	730	mobile (steps)	9.91, ≈10.04
(c)	Ag(110)	intermediate,		mobile (islands)[h]	10.07, 10.23[i]
	Ag(111)[j]	predominantly	770	mobile (steps)	≈10
	Au(110)	ionic	800[k]	mobile (steps)[l]	10.04[m]
	Au(111)[j]		770	mobile (steps)	≈10
	Cu(110)[n]		730		9.7−11.1
	Cu(111)[o]			mobile (steps)	10.1
(d)	Si(100)	Strong,	dissoc.[e] at 1070 K	immobile[o]	9.87, 11.58[p]
	Si(111)	predominantly	dissoc.[q] at 1100 K	immobile[r]	
	Ge(111)[s]	covalent	970	immobile	14.4
	Ge(100)[p]				9.6, 11.52
	Ni(110)		dissoc.[t] at 760 K	reduced mobility[u]	10,[n] 10.5,[n] ≈11.6[u]
	Pt(111)[v]		dissoc. at 1050 K	low mobility	10.0±0.3

[a]From Ref. 7.
[b]From Ref. 24.
[c]From Ref. 6.
[d]From Ref. 10.
[e]From Ref. 8.
[f]Present work. See Sec. III C 1 for a detailed discussion of the indicated bond lengths.
[g]From Refs. 25, 26, 27, and present work.
[h]From Ref. 3.
[i]From Ref. 28.
[j]From Ref. 14.
[k]From Ref. 15.
[l]From Ref. 2.
[m]From Ref. 29.
[n]From Ref. 30.
[o]From Ref. 31.
[p]From Ref. 32.
[q]From Ref. 33.
[r]From Ref. 34.
[s]From Ref. 35.
[t]From Ref. 36.
[u]From Ref. 17.
[v]From Refs. 36 and 37.

Scanning tunnelling microscopy (STM) has played a central role in determinations of overlayer structures formed upon adsorption of C_{60} on this group of surfaces,[38] for which the bond to the fullerenes is predominantly ionic. From observation of the growth of submonolayer quantities of C_{60}, it has become clear that at coverages of a few percent of a full monolayer, the molecules are mobile at room temperature, selectively decorating the step edges on Ag(111),[14,39] Au(110),[2] Au(111),[39,40] and Cu(111).[31] C_{60} forms two-dimensional islands on Ag(110),[3,28] although it is not clear if this occurs already at room temperature due to the annealing treatment used there. These results are summarized in column 3 of Table I. Ordered or partially ordered monolayers have been produced on all of these substrates by annealing films, typically to temperatures around 700 K, and at least some degree of commensurability is always observed, indicating the increasing substrate-adsorbate bond strength. Further evidence for the enhanced strength of this interaction compared to the inert surfaces discussed above comes from observed reconstruction of many of these metallic substrates. E.g., on Au(110) both the C_{60} molecules and Au atoms take part in a reconstruction resulting in (6×5) overlayer,[2] while on Au(111) the unusual $(23\times2\sqrt{3})$ reconstruction is modified upon C_{60} adsorption.[41,14] As shown in row (c), column 4

of Table I, however, the NND's for the lowest-energy equilibrium structures remain close to the solid C_{60} value (10.04 Å), so that the effect of the adsorbate-adsorbate interaction is still significant. We have observed that for C_{60}/Au(110),[1] in addition to the charge transfer discussed above, the molecular orbitals of the fullerene are hybridized with the substrate bands. A full understanding of the bonding for this system therefore also requires consideration of the perturbation on the molecular electronic structure due the chemical interaction with the substrate.

Finally, in row (d) of Table I is a group of metal and semiconductor substrates that bond much more strongly to C_{60}. For these systems, the bonding is predominantly covalent in character.[42,43,35,36] The substrate-adsorbate interaction now tends to dominate, and on Si(111), Si(100), and Si(110) surfaces, the first-layer C_{60} molecules are immobile at room temperature.[43–45] This is also the case for Ge(111),[35] while on Pt(111)[36] and Ni(110),[17] the surface mobility is more restricted than for Au, Ag, and Cu. Another consequence of the increased strength of the substrate-adsorbate bond is that the deviation in the C_{60}-C_{60} separation from the solid C_{60} value is greater for the equilibrium stuctures formed on these substrates. Values ranging from 9.6 Å (a decrease of 5%) for the shortest C_{60}-C_{60} separation on Ge(100)[32] to 14.4 Å (an increase of 43%) for the lowest-energy phase on Ge(111)[35] have been quoted. In these cases the fullerene molecules are forced into commensurate structures.

High-resolution electron energy-loss spectroscopy (HREELS) and PES results obtained for C_{60} layers on Pt(111) (Ref. 36) show that, in common with Si(100),[8] Si(111),[33] and Ni(110),[17] the bond strength is sufficient to catalyze the decomposition of the fullerenes into a carbidic layer at the temperatures given in column 2 of Table 1. In the case of Ge, however, C_{60} desorbs intact from the (111) surface, although the temperature at which this occurs (970 K),[35] is actually higher than that at which C_{60} dissociates on Ni(110). As indicated in Table I, the substrates discussed here can be classified into the following categories: weak, predominantly van der Waals bonding; intermediate, predominantly ionic bonding; and strong, predominantly covalent bonding.

In the present paper, we focus on Al(111) and Al(110), and by combining the results presented here with our preceding studies, we find that in terms of the classifications given above, a new category of intermediate covalent bonding must be added to describe the interaction between C_{60} and Al. Considering the characteristics of these systems in the order given in Table I, we find the following: (1) As reported previously,[25] the bonding for an annealed monolayer of C_{60} on Al(111) is covalent, which is also true for the two new phases reported here; (2) the desorption temperature for a ML on both of these Al surfaces is ~730 K; (3) we show elsewhere using STM that the molecules are mobile at room temperature on Al(111);[27] and (4) C_{60}-C_{60} bond lengths for these surfaces vary from 9.91 Å to 12.13 Å.

This paper is organized as follows: we present the experimental details in Sec. II. To simplify the organization of the primary information gained with each experimental technique we combine results and discussion in Sec. III. Section III A is devoted to structural characterization [low-energy electron diffraction (LEED) and Al $2p$ PES], and Sec. III B primarily to information on the electronic states (valence PES, C $1s$ XAS and C $1s$ PES), including work function measurements. Some structural information is also derived there from XAS. More detailed discussion follows in Sec. III C, and we draw conclusions in Sec. IV.

II. EXPERIMENTAL DETAILS

PES and XAS data were taken at Beamline 22 of MAX-lab, using a modified SX700 monochromator and a high-efficiency electron spectrometer.[46] Films were evaporated onto clean Al(111) and Al(110) substrates from a Ta crucible ($T \approx 300$ °C) with pressures in the low 10^{-10} mbar range. Ordered monolayers were produced by evaporating C_{60} while the Al(111) and Al(110) surfaces were held at a temperature of 620 K. Since this temperature is well above the evaporation temperature of solid C_{60}, only one monolayer sticks to the surface,[1] and evaporations can be made until the coverage, as measured by the C $1s$ PES intensity, saturates. We define this to be 1 ML, which corresponds to 1/12 of the Al surface atomic density (see Figs. 2 and 15). While this method was used for all the films studied on Al(110), some films produced on Al(111) were also made with T_{sample}=RT. These films represent less than a full ML, since non-layer-by-layer growth occurs at this temperature, and to be sure that all molecules studied were in direct contact with the substrate less than a complete layer was deposited. Confirmation that no second or higher layers were present came from C $1s$ PES, for which multilayer growth is observed to result in a new component at higher binding energy.[47,1] XAS was measured by recording the total electron yield as a function of photon energy above the C K edge, with a photon energy resolution of 150±50 meV. Photon energy calibration was carried out by measuring the kinetic energy shift of the Al $2p$ spectrum excited with first- and second-order light. For the Al $2p$, valence, and C $1s$ PES data, the total experimental resolutions were 60±20 meV, 120±40 meV, and 240±50 meV, respectively. Work-function measurements were carried out according to procedures described in detail elsewhere.[47] All measurements were made at 300 K, and all the PES data were recorded in normal emission.

III. RESULTS AND DISCUSSION

A. Physical structure

1. Ordered C_{60} monolayers on Al(111)

a. LEED. Upon deposition of C_{60} onto Al(111) at room temperature, a $(2\sqrt{3}\times 2\sqrt{3})R30°$ LEED pattern is observed. Patterns obtained for ML-covered and clean Al(111) are shown in Fig. 1. Pattern 1(b) corresponds to a hexagonal overlayer with a NND of 9.91 Å, ≈1.1% less than that of solid C_{60} at 300 K (NND=10.02 Å), but very close to the value for the orientationally ordered low-temperature phase (NND=9.93 Å).[48] A model of this phase showing the unit cells of substrate and adsorbate is presented in Fig. 2. Identical but weaker LEED patterns were also obtained for several coverages as low as 0.25 ML; coverage calibration was carried out by comparison of the C $1s$ PES intensity to that obtained from a saturated (6×6) monolayer, or by using STM.[27] All molecules in a $(2\sqrt{3}\times 2\sqrt{3})R30°$ structure have

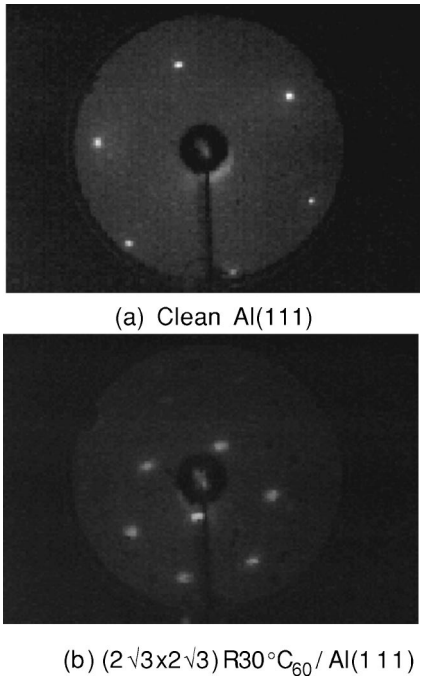

FIG. 1. LEED patterns for the following surfaces: (a) clean Al(111) (electron energy=118 eV) and (b) 0.9±0.1 ML $(2\sqrt{3}\times2\sqrt{3})R30°$ C_{60}/Al(111) (electron energy=27 eV).

a one-to-one correspondence with molecules in a (6×6) overlayer, i.e., transformation of the former to the latter can be accomplished in the present case by raising every third molecule. We find that this room-temperature-evaporated phase is in fact metastable, with a phase transformation occurring upon annealing the sample at 490 K, after which the (6×6) LEED pattern is observed. Details on the growth of this phase are given elsewhere.[27]

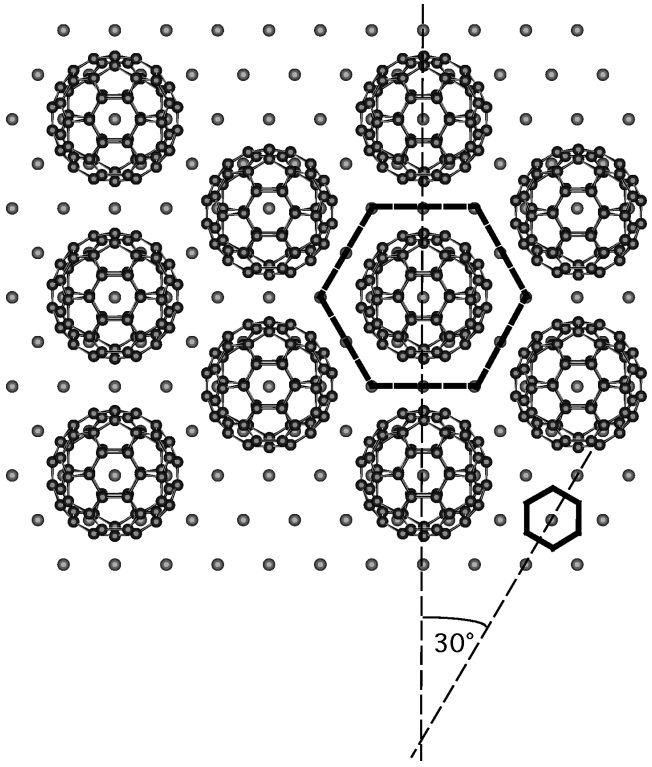

FIG. 2. A model of the $(2\sqrt{3}\times2\sqrt{3})R30°$ phase. The dashed hexagon encloses an overlayer-induced unit cell, while the solid hexagon encloses a unit cell of the Al(111) surface.

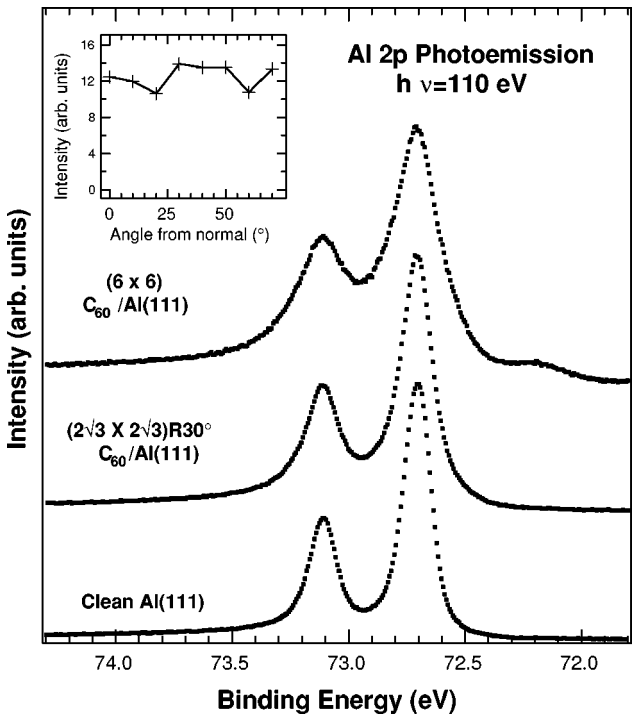

FIG. 3. Al 2*p* PES for the samples indicated. For all three samples, the $J=3/2$ and $J=1/2$ components of the spin-orbit split doublet have binding energies at 72.71±.01 eV and 73.11±.01 eV, respectively, which is in good agreement with previously reported measurements on the clean surface (Ref. 49). The line is broadened from a full width at half-maximum (FWHM) of 0.14 eV for the $J=3/2$ component on clean Al(111) to 0.17 eV for the $(2\sqrt{3}\times2\sqrt{3})R30°$ phase and 0.26 eV for the non-reconstructed component of the (6×6) phase. The new feature observed at 72.2 eV in the (6×6) data has been assigned previously to Al atoms taking part in the substrate reconstruction accompanying the formation of this equilibrium phase (Refs. 25 and 26). Inset: Area of the reconstruction-induced peak for the (6×6) spectrum as a function of electron emission angle with respect to normal.

b. Al 2p PES. We present in Fig. 3 Al 2*p* PES for $(2\sqrt{3}\times2\sqrt{3})R30°$ C_{60}/Al(111), (6×6) C_{60}/Al(111), and the clean substrate. The feature for the (6×6) sample at 72.2 eV has been discussed previously, and we assign it to Al atoms taking part in the reconstruction of the substrate accompanying the formation of the (6×6) structure.[25] That this peak is not present in the $(2\sqrt{3}\times2\sqrt{3})R30°$ spectrum is consistent with this interpretation. The broadening in the $(2\sqrt{3}\times2\sqrt{3})R30°$ spectrum compared to that of clean Al(111) is evidence of a bonding interaction that perturbs the chemical environment at the interface. The Al 2*p* binding energy is influenced by both the initial-state charge density and the final-state screening properties, both of which will vary depending on the proximity of the Al atom to the C_{60} overlayer. From Fig. 2 it is clear that, due to the large size of the fullerene molecules, there are a variety of different Al-C distances depending on which Al atom is probed, and we assume that this accounts for the observed broadening.

The inset in Fig. 3 shows the variation in the intensity extracted from curve fitting of the reconstruction-induced

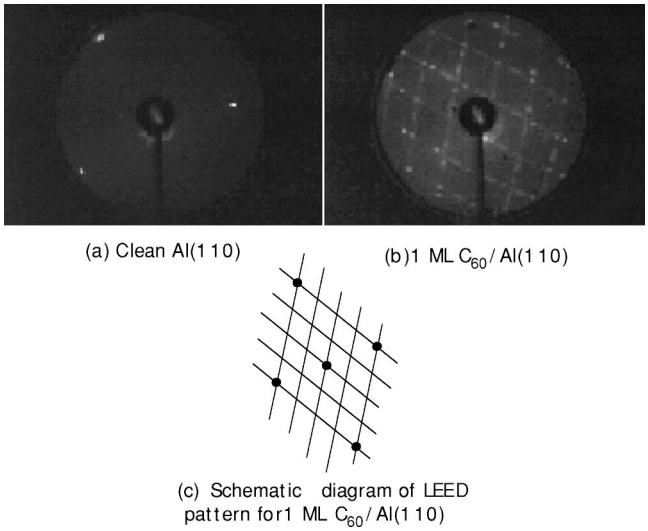

FIG. 4. LEED patterns (electron energy=47 eV) for clean Al(110) and for 1 ML C_{60}/Al(110) evaporated with the substrate at 620 K. The adsorbate-induced pattern is a set of lines forming a grid, for which the points of intersection of the lines are the points at which spots would be observed in a $c(4\times4)$ pattern. The lines indicate a lowering of the total symmetry along the given direction in the overlayer.

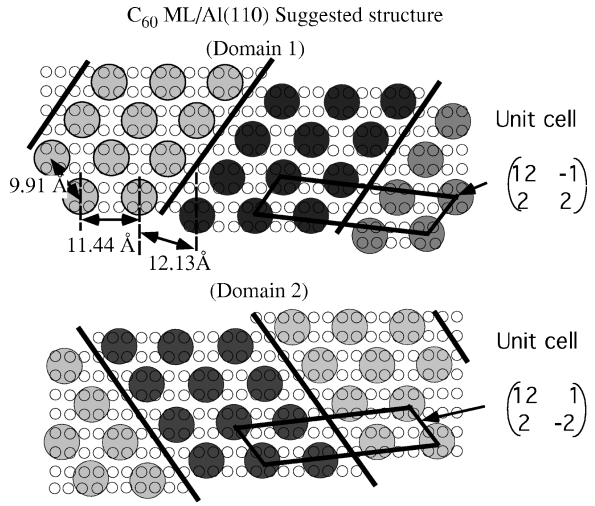

FIG. 5. A model of the proposed structure for 1 ML C_{60}/Al(110). The single slanted lines in the figure are domain boundaries; within each domain the molecules form a $c(4\times4)$ overlayer, and the entire overlayer structure is displaced by one atomic row across each domain boundary. The solid parallelograms show the two possible types of unit cell, corresponding to the two possible directions for domain boundaries as shown, and explaining the netlike LEED pattern.

peak for 1 ML (6×6) C_{60}/Al(111) as a function of emission angle. Based on normal emission data, we previously estimated that the feature observed at 72.2 eV resulted from one in six Al interface atoms. By measuring the angular variation of the Al $2p$ lines we are able to check the effect of possible photoelectron diffraction on the relative intensities of these peaks, and give a more reliable estimate of the number of atoms producing the reconstruction-induced peak. The data have been modeled using two sets of Voigt functions representing the two spin-orbit doublets, where the ratio of the two components in each doublet and the associated spin-orbit splitting is identical. The areas obtained, together with previous calculations of the substrate mean free path,[50] allow us to revise our previous estimate, and state that a maximum of eight atoms per unit cell are affected. We note that any displacement of these Al atoms away from the surface could well enhance their contribution to the spectra away from normal emission, and that these results are fully consistent with 6–7 atoms directly below each displaced molecule in the (6×6) structure being partially drawn away from the surface, as suggested previously.[25]

That the (6×6) reconstruction-induced Al $2p$ component should correspond to atoms that are drawn away from the surface, rather than the effect of a chemical shift, is suggested by the fact that this component is separated from the main line by a full 0.55 eV.[25] It is thus not part of the continuum of environments suggested by the broadening of the main line. This has been confirmed via the effects on the molecularly resolved density of states (DOS) by scanning tunnelling spectroscopy (STS),[26] and we discuss this in more detail in Sec. III C 1.

2. Ordered C_{60} monolayer on Al(110)

a. LEED. In Fig. 4 LEED patterns for clean Al(110) and 1 ML C_{60}/Al(110) are shown, as well as a schematic diagram representing the LEED pattern for the C_{60}-covered sample. The pattern for the C_{60}-covered sample consists of a series of spots lying close together in a grid, in which the points of intersection of the lines of spots forming this grid are at the same position as the spots would be in a $c(4\times4)$ LEED pattern. The pattern observed indicates the presence of a lowering of the total symmetry along one direction in the overlayer. Our proposed structure for this system is shown in Fig. 5; it consists of a series of stripelike domains in which $c(4\times4)$ periodicity occurs, separated by domain boundaries across which the overlayer structure has shifted by one atomic row. In order for the present LEED pattern to be observed, the presence of domain boundaries occuring in the two distinct directions indicated in the figure is required. A description of the unit cell requires matrix notation, and an example for a domain width of three molecular rows is shown in Fig. 5. The full notation for the proposed overlayer structure is

$$\begin{pmatrix} 4n & \pm 1 \\ 2 & \mp 2 \end{pmatrix},$$

where n is the number of molecular rows defining the domain width.

The existence of somewhat regular superstructure spots in the LEED pattern suggests that there might exist one or more favored domain widths. It is also possible, however, that the pattern shown represents a metastable overlayer, since we have not optimized the kinetic factors for this surface. Slight variations in the superstructure spot positions and intensities were observed among the LEED patterns for different preparations. Nevertheless, the persistent lack of uniform streaking in the pattern is consistent with the idea of stable domain widths. We return to this point in Sec. III C 1.

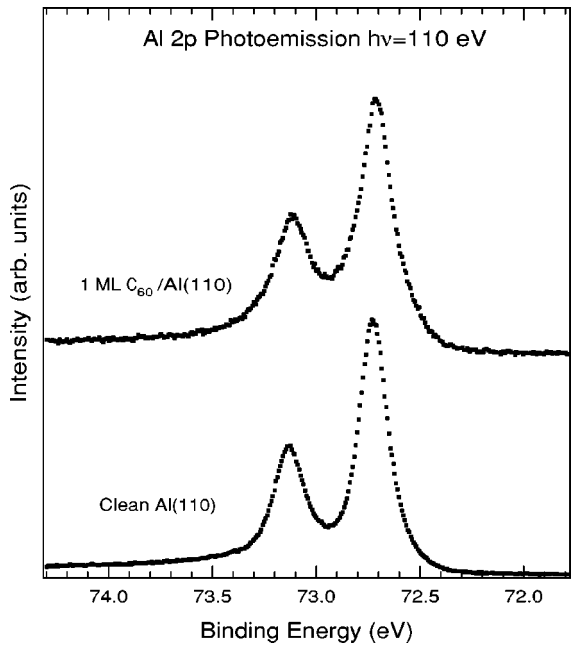

FIG. 6. Al $2p$ PES for clean Al(110) and for 1 ML C_{60}/Al(110) using a photon energy of 110 eV. The binding energy of the $J=3/2$ component is 72.71 eV, which is identical for both samples. The spectrum is broadened upon adsorption of C_{60}, with the FWHM of the $J=3/2$ component increasing from $0.17\pm.01$ eV to $0.20\pm.01$ eV.

b. Al 2p PES. Al $2p$ PES data for 1 ML C_{60}/Al(110) and for clean Al(110) are shown in Fig. 6. As for the $(2\sqrt{3}\times 2\sqrt{3})R30°$ phase on Al(111), shown in Fig. 4, the spectrum for the 1 ML C_{60}/Al(110) phase shows a distinct broadening compared to that of the clean Al(110) substrate. Again, this is evidence of the chemical bond formed between C_{60} and the substrate. However, no new feature of the type observed for the (6×6) phase is seen in the spectrum, indicating that no such reconstruction occurs on Al(110). This is consistent with our interpretation of the LEED pattern, in that the symmetry reduction is achieved via displacement of molecules in the plane of the surface, rather than perpendicular to it as on Al(111).[25,26]

B. Electronic structure of C_{60} monolayers on Al

In this section we describe measurements of the electronic structure of the C_{60} monolayers described above. Valence PES and C $1s$ XAS give a consistent picture of the characteristics of the adsorbate-substrate interaction and the relative bonding strength. PES is used to show as closely as possible the effects on the DOS of adsorption on Al, including effects near E_F. Since a direct comparison of the relative bond strengths based on an analysis of the widths of valence features as seen in PES is complicated by the fact that we measure a combination of adsorbate and substrate emission, we employed core level techniques. The core-level spectroscopies XAS and XPS/PES (Ref. 51) (including shakeup) give site-specific information about the core-excited state, and allow the possibility to study the adsorbate alone. Furthermore, because the core hole is relatively well screened by the molecule,[52] we expect the spectra to reflect the general bonding trends. To emphasize the connections between the various results, we will compare the spectra from the different systems obtained with each technique as it is introduced.

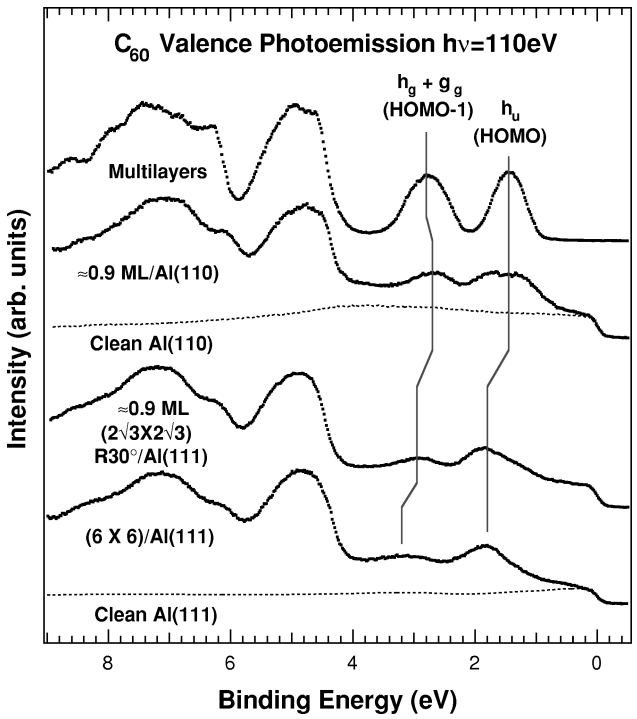

FIG. 7. Valence PES at a photon energy of 110 eV is shown for the samples indicated. No new feature at the E_F due to partial filling of the t_{1u} level, of the type observed previously on Cu, Au, and Ag, is present in the ML spectra on Al. For all three monolayer phases, the HOMO and HOMO-1 are considerably broadened compared to the case of C_{60} multilayers.

1. Valence PES

Valence PES data for 1 ML C_{60}/Al(110), 1 ML $(2\sqrt{3}\times 2\sqrt{3})R30°$ C_{60}/Al(111), 1 ML (6×6) C_{60}/Al(111), clean Al(111), and Al(110) are shown in Fig. 7. The first two C_{60}-induced peaks are labeled according to their molecular symmetry.[53] The $5h_u$-derived band will from now on be referred to as the highest occupied molecular orbital (HOMO) and the $(7h_g, 5g_g)$-derived bands as the HOMO-1. The spectra for the three monolayer phases on Al also include contributions due to emission from the substrates. For clean Al this is essentially featureless with a relatively low cross section, as seen from the figure. This facilitates a simple identification of C_{60}-derived features, and makes interpretation of the data easier than for previous valence PES measurements on C_{60} monolayer systems.[1,19,21,36,54–57] No new feature is observed at E_F for any of the phases on Al, and the HOMO and HOMO-1 are considerably broadened compared to solid C_{60} in all three cases. As discussed previously for the (6×6) phase,[25] this is strong evidence for covalent bonding. It is thus clear from the present results that covalent bonding also occurs for $(2\sqrt{3}\times 2\sqrt{3})R30°$ C_{60}/Al(111) and 1 ML C_{60}/Al(110).

In Fig. 8 we present valence PES data for the three ordered phases of C_{60} on Al, recorded at a photon energy of 80 eV, from which a background due to the relevant Al substrate has been subtracted. Since an exact determination of the background contribution is not possible, the maximum

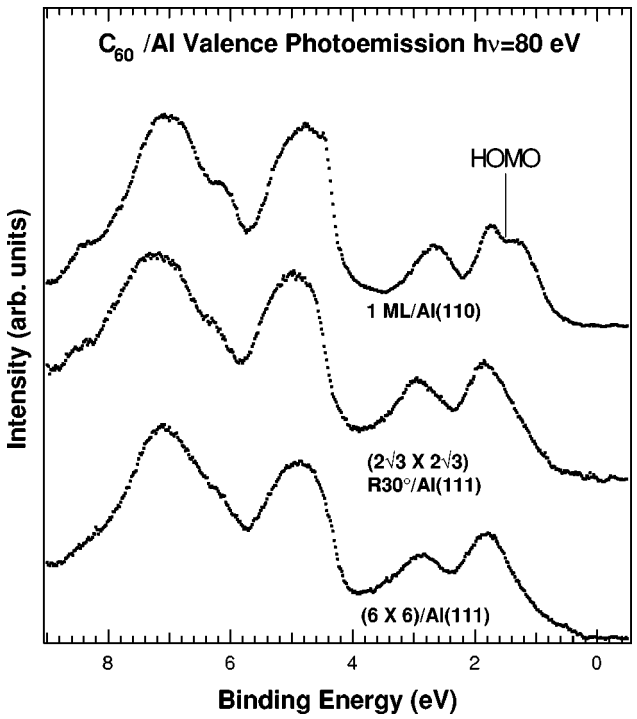

FIG. 8. Valence PES for the samples indicated, taken at a photon energy of 80 eV. Backgrounds have been subtracted as described in the text. The presence of two components in the HOMO for 1 ML C_{60}/Al(110) is clear, and the shape of the HOMO for the $(2\sqrt{3}\times 2\sqrt{3})R30°$ and (6×6) phases on Al(111) suggests that such a component is present, but greatly broadened.

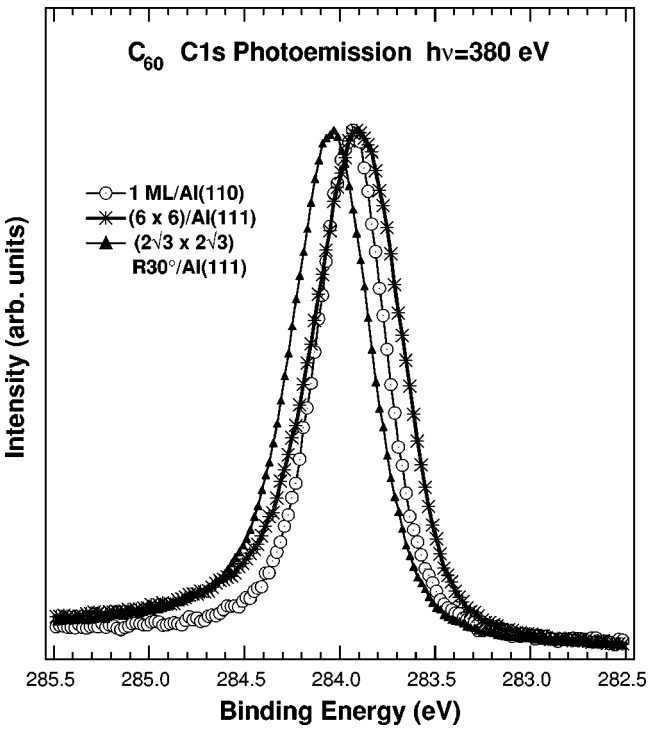

FIG. 9. C 1*s* PES for the samples indicated. The positions and widths of the lines are given in Table II.

background which does not result in zero intensity has been removed. We note that for all three phases the C_{60}-induced DOS stretches to the Fermi level. It is particularly obvious from the presence of more than one distinct feature in the spectrum for C_{60}/Al(110) that the fivefold degeneracy of the HOMO is split by the symmetry breaking interaction with the surface. A similar effect is observed for C_{60}/Al(001),[58] and also suggested by data for Ag(110).[59] The apparent narrowness of the feature observed at 1.7 eV binding energy indicates that one or more of the HOMO-derived orbitals is interacting more weakly with the substrate than the others. The cross section of this feature is seen to vary strongly with photon energy in a manner similar to the HOMO of solid C_{60}. A careful examination of the low-energy side of the HOMO for the (6×6) and $(2\sqrt{3}\times 2\sqrt{3})R30°$ phases on Al(111) reveals the presence of a shoulder which could also be derived from splitting in the HOMO, with the stronger bonding broadening this feature. This broadening is found to be site-dependent for the (6×6) overlayer using STS.[26]

2. C 1s PES and shakeup

In Fig. 9 we present C 1*s* PES results for the three monolayer phases on Al. The main line binding-energy positions and widths are given in Table II. We note that the observed widths are much lower than, e.g., found for high-resolution studies of C_{60}/Au(110),[1] C_{60}/Cu(001),[22] C_{60}/Ag(111),[37] and K fullerides.[60,61]

The shakeup spectra for these three phases are compared to that of solid C_{60} in Fig. 10, where the binding-energy scale shown is relative to the main line. These features can be understood to derive from final states of the core-ionized C_{60} molecule in which one electron has been promoted from the occupied to the unoccupied valence band.[62] The structures observed therefore represent a convolution of the occupied and unoccupied levels, with modifications due to the core hole; see also the discussion in Sec. III B 3. While all the monolayer spectra show broadening compared to the solid C_{60} data, the shakeup features observed for the two C_{60} phases on Al(111) are considerably broader than for 1 ML C_{60}/Al(110). There is also a slight increase in width going from the $(2\sqrt{3}\times 2\sqrt{3})R30°$ phase to the (6×6) phase on Al(111). These data therefore give direct evidence of the increase in C_{60}-Al interaction strength in the series 1 ML C_{60}/Al(110), $(2\sqrt{3}\times 2\sqrt{3})$ C_{60}/Al(111), (6×6) C_{60}/Al(111), confirming the trend observed in the XAS and valence PES data.

3. X-ray absorption spectroscopy

In Fig. 11 we present XAS data for the three ordered C_{60} monolayer systems on Al, comparing them to 1 ML C_{60}/Au(110) (Ref. 63) and solid C_{60}. The broadening observed in the π^* levels (between 283 and 290 eV) is consistent with geometrical changes expected to be associated with covalent bonding, as is the shift of the LUMO to higher

TABLE II. C 1*s* binding energy and FWHM for the indicated samples.

Sample	Binding energy (eV)	FWHM (eV)
1 ML/Al(110)	283.93±0.05	0.43
$(2\sqrt{3}\times 2\sqrt{3})R30°$	284.05±0.05	0.49
(6×6)	283.90±0.05	0.55

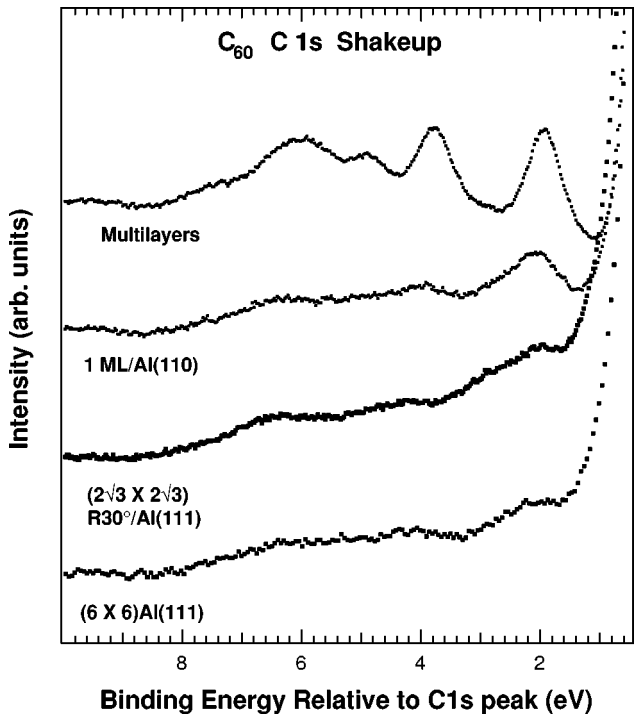

FIG. 10. C 1*s* shakeup spectra, for which the binding energy scale is given relative to the center of the main line. The observed broadening reflects hybridization of the occupied and unoccupied states of C_{60} with the substrate bands, and follows the sample dependence observed in XAS.

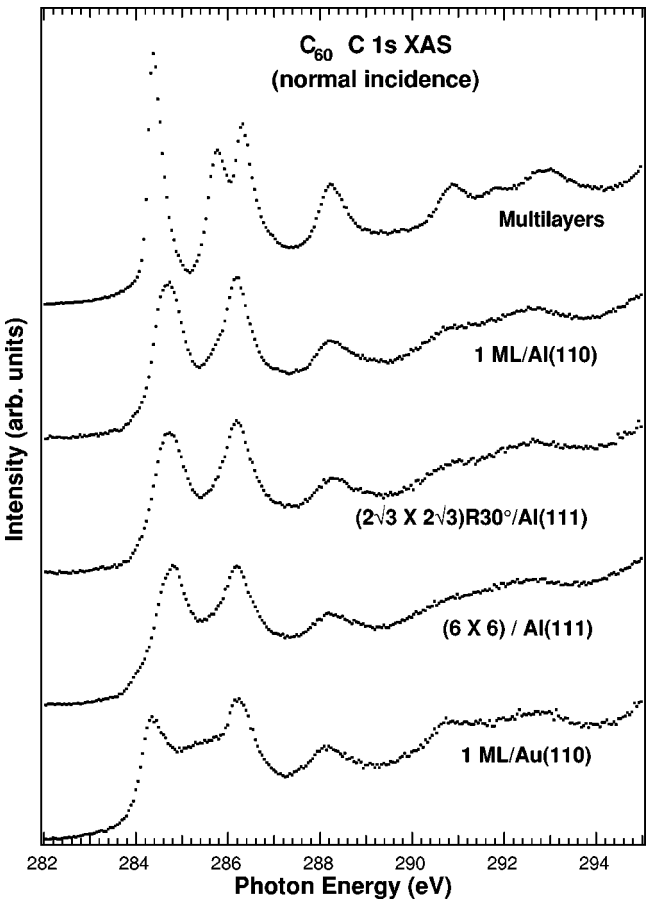

FIG. 11. C 1*s*-XAS data for the samples indicated. The C 1*s* ionization potential ($\sim$289.5 eV, see below) separates the spectra into two primary parts: the structure below this energy is due to predominantly π^*-derived unoccupied bound states whose σ^* character increases as they approach this energy, while above the ionization potential the features are often described alternately as σ^* states, or in terms of scattering of the outgoing electron by the atoms within the core-ionized molecule. The pattern of increased broadening in the series 1 ML C_{60}/Al(110), $(2\sqrt{3}\times 2\sqrt{3})R30°$/Al(111), (6×6)/Al(111) reflects changes in the electronic and physical structure due to the covalent bond. The C 1*s* ionization potentials are as follows: Solid C_{60}, 289.60 eV (Ref. 47); 1 ML/Al(110), 289.2 eV; (6×6), 289.05 eV; $(2\sqrt{3}\times 2\sqrt{3})R30°$, 289.20 eV; 1 ML/Au(110), 289.1 eV (Refs. 18 and 1). For the monolayers we take the E_F-referenced binding energy (Table II) and add the work function (Table IV).

energies. This is similar to the effects of photopolymerization.[64] The features observed above the C 1*s* ionization potential, which is near 289.5 eV relative to the vacuum level in all cases (see figure caption), can be understood in terms of scattering of the excited electron by the surrounding atoms. These are often described as σ^* resonances.[65] We have previously related broadening in these scattering-derived features to distortions in the molecular structure induced by the covalent bonding between C_{60} and Al.[25] We would like to point out that the data in Fig. 11 for the (6×6) case replace those published previously,[25] which were overly broadened due to normalization difficulties. Common for all three phases of C_{60}/Al is that the LUMO+1 and LUMO+2 resonances cannot be resolved, and a peak derived from both these structures is observed at 286.15±.05 eV. The LUMO resonance is shifted to a higher energy compared to solid C_{60}, and the energy and width of this feature for the three samples is summarized in Table III.

Both the π^*- and σ^*-derived features become progressively broader in the series 1 ML C_{60}/Al(110), $(2\sqrt{3}\times 2\sqrt{3})$ C_{60}/Al(111), (6×6) C_{60}/Al(111). The broadening observed in the π^*-derived levels has previously been assigned to increased hybridization between the molecular orbitals of core-excited C_{60} and the substrate;[25] this is discussed in more detail elsewhere.[66] We do not expect the character of the bonding to differ significantly due to effectively replacing one C atom (that which is excited by the x-ray photon) with N ($Z+1$ approximation), since the great majority of the excitations involve a C atom not in direct contact with the surface.[66] It is therefore of significant interest that the shift to higher energy of the LUMO follows the increase in bond strength.[67] As shown in Fig. 12, angle-dependent spectra show an interesting trend of greater broadening and increased energy of the LUMO resonance with more normal incidence as well. This confirms the trend shown in Table III in another way, since it corresponds to an

TABLE III. C 1*s*-to-LUMO XAS resonance energy and FWHM for the indicated samples.

Sample	Photon energy (eV)	FWHM (eV)
1 ML/Al(110)	284.65±0.05	0.70
$(2\sqrt{3}\times 2\sqrt{3})R30°$	284.70±0.05	0.75
(6×6)	284.80±0.05	0.80

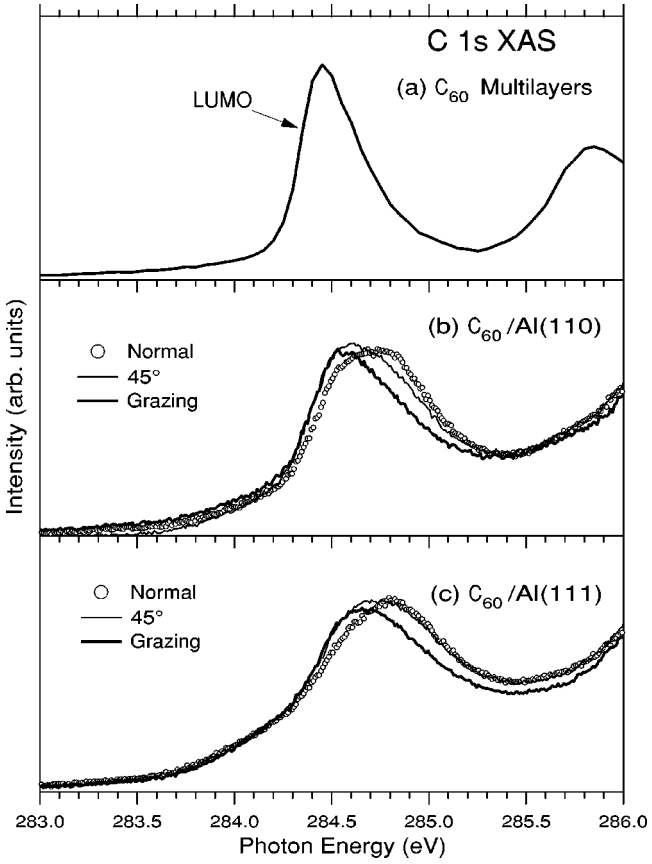

FIG. 12. C 1*s*-XAS data at the LUMO resonance for the samples indicated, showing in detail the evolution of the spectra as a function of the indicated incidence angles. The observed variation is due to a varying chemical interaction of the LUMO wave function with the substrate, as described in the text. A similar variation was observed for the $(2\sqrt{3}\times 2\sqrt{3})R30°$ phase, but is not shown due to poorer statistics.

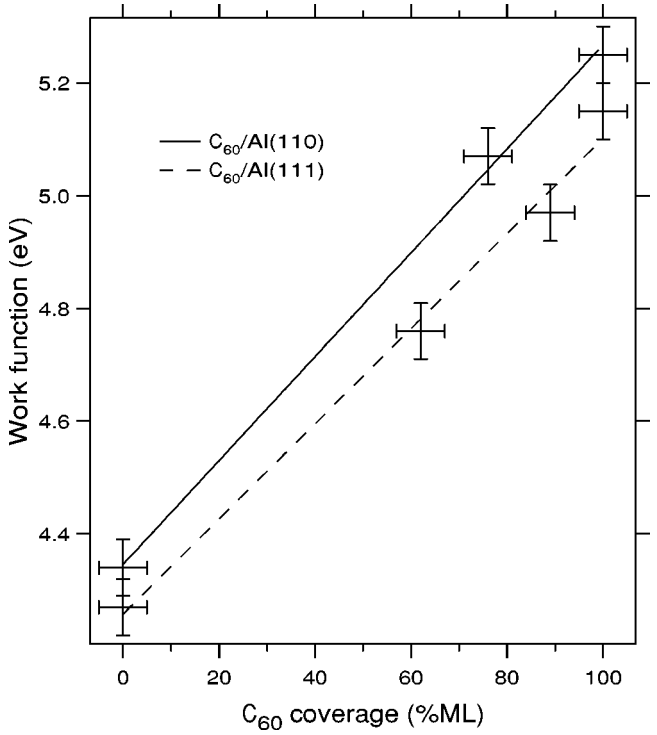

FIG. 13. Measured work-function changes upon C_{60} adsorption on Al(110) and Al(111). The data for 0 and full ML coverage correspond to those given in Table IV, with the samples prepared at 620 K. The same preparation was used for the submonolayer on Al(110), whereas the submonolayer samples on Al(111) were prepared at room temperature. The linear fit is discussed in the text.

increasing (but still moderate) overlap of the LUMO-resonance wave function with the substrate.[66]

4. Work functions

One often associates the change in work function of a metal surface upon the adsorption of an atomic or molecular species with a change in the surface dipole.[68] It is difficult to place C_{60} into a previous model for adsorbates when considering what kind of surface dipole layer one should expect this three-dimensional adsorbate to form. For a noble gas, e.g., the ground-state interaction with the substrate is weak, but the chemical interaction of excited states appears to have a determining role in the size of the dipole formed, and thus the work function change.[69] An atomic adsorbate such as an alkali metal, which is very likely to donate charge in the ground state due to its very low ionization potential, lowers the work function of most metal substrates.[68] Adsorption of oxygen, which has a high electron affinity of 3.1 eV,[70] has variable effects, but has a tendency to raise the work function of metals.[68] C_{60} has certain characteristics in common with Xe, i.e., its large size, the fact that it is a closed-shell system, and that the bonding of the solid can be described as largely van der Waals. It has a gas phase ionization potential (7.6 eV) (Refs. 71,7) that is large compared to most metal surface work functions, and a reasonably large electron affinity (2.7 eV).[72] Thus C_{60} is not expected *a priori* to donate electrons to metal surfaces, whereas the question of how many it will accept is a more difficult issue. At the same time, it is a large adsorbate with many possible internal excitation channels, so that it might behave differently than all of the above. Combining our data for the present systems with previous data for C_{60}/Au(110), this is in fact what we observe.

In Fig. 13 we show the evolution of the work function for C_{60} submonolayers on Al(111) and Al(110) as a function of coverage. This function is linear for the few data points we have. A linear coverage dependence is consistent with the trend for Xe adsorbed on simple metal surfaces,[69] but the positive shift is not. We compare the results of previous and present work function measurements for monolayer C_{60}-covered metal substrates in Table IV. It is clear that the positive shift measured on Al surfaces is also opposite to the case for C_{60}/Au(110) (Ref. 18) and C_{60}/Cu(111).[20] As we see in the present paper, C_{60} bonds covalently to Al surfaces, while there is a significant charge transfer to the fullerene on Au(110) (Refs. 16,18) and charge transfer has been observed elsewhere from Cu(111) to C_{60}.[20] The work function of clean Au(110) is slightly over 5 eV, whereas the work functions for the Al surfaces are less than 4.5 eV. Thus, charge transfer to C_{60} involves a strong lowering of the work function on Au(110) (contrary to the dipole model), whereas the covalent bonding cases involve a large increase. A work-function decrease on Rh(111) was used to conclude that charge was transferred in the opposite direction, i.e., from C_{60} to Rh.[57] This interpretation seems unlikely to be correct, however,

TABLE IV. Work-function measurements for C_{60} monolayers on metal substrates. Values quoted in parentheses for the clean substrates are taken from references other than the works in which the C_{60}-overlayer measurements were presented, as indicated.

Sample	Clean sample Work function (eV)	Work function with C_{60} ML (eV)	Difference (eV)
Al(110) [a]	4.35±0.05[b]	5.25±0.05	+0.95±0.07
Al(111)[a]	4.25±0.05[c]	5.15±0.05	+0.95±0.07
Au(110)[d]	(5.37)[e]	4.82±0.05	−0.45±0.05
Cu(111)[f]	5.4	5.0	−0.4
Ni(111)[f]	5.02	5.17	+0.15
Rh(111)[g]	(5.40)[h]	4.95	−0.35
Ta(110)[i]	(4.80)[e]	5.4	+0.6

[a]Present work.
[b]A value of 4.28±0.02 eV was reported in Ref. 73, and is close to a recent theoretical value (Ref. 74).
[c]A value of 4.24±0.02 eV was reported in Ref. 73.
[d]From Ref. 18.
[e]From Ref. 75.
[f]From Ref. 20.
[g]From Ref. 57.
[h]From Ref. 76.
[i]From Ref. 55.

when one considers the ionization potential of C_{60}, and the observed behavior for the Au(110) and Cu(111) cases. We have no conclusive explanation for these results, but note only that C_{60} adsorbed on a metal surface appears to have a work function close to 5 eV in all cases studied thus far. This is a pattern that is consistent with a three-dimensional overlayer, such that the nature of the chemical bond at the interface contributes at most a correction term to the fundamental dielectric response of the C_{60} overlayer.

C. Further aspects of the C_{60}-Al interaction

1. Energetics of equilibrium monolayer structures

Here we propose explanations for the structures adopted by the overlayers on the two substrates studied here. In the absence of detailed structural determinations (e.g., x-ray diffraction), we attempt to reach sensible models based on the available data. We start with the case of $c(4\times4)$ C_{60}/Al(110), using the LEED and Al $2p$ PES data, and then develop the discussion of the (6×6) that was begun in Ref. 26, and thus obtain a consistent picture.

In order to justify the structure proposed in Sec. III A 2 for the equilibrium ML on Al(110), the following simple arguments based on energetics appear to be useful. Considering the equivalent structure and the almost exactly equal bond distances for Ag(110) and Al(110), it is interesting to note that $c(4\times4)$ domains were observed in STM studies of C_{60} monolayers on the former surface.[28,3] Within a $c(4\times4)$ overlayer of C_{60}/Al(110) there would be two NND's, 9.91 Å and 11.44 Å as shown in Fig. 5. Since 9.91 Å is somewhat shorter than the van der Waals bonding distance for solid C_{60}, a stress would be inherent in the overlayer for the true $c(4\times4)$ structure.[77] Thus we are led to consider the energetics of C_{60} adsorption at the boundary of a $c(4\times4)$ domain. Figure 14 illustrates the possible adsorption positions.[78] Apart from the continuation of the $c(4\times4)$ phase, the next most favorable position in terms of producing bond distances as close to the solid C_{60} NND as possible is one in which the adsorbed molecule has shifted one atomic row with respect to the original $c(4\times4)$ domain. As soon as one molecule has adopted such a shifted position, additional fullerenes adsorbing around it will take on $c(4\times4)$ positions in a new domain.

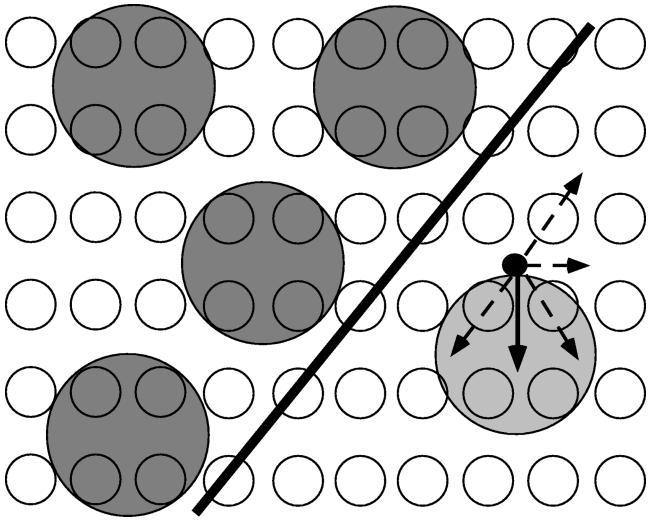

FIG. 14. Depiction of the adsorption of a C_{60} molecule in a shifted-row position at a domain boundary on Al(110). The small black circle marks the adsorption position, which would continue the $c(4\times4)$ structure. The arrows indicate possible minimal shifts to equivalent bonding sites [the site shown is arbitrary, but equivalent to the ones indicated for the $c(4\times4)$ domain]. The shift of one atomic row shown and indicated by the solid arrow is the most favorable, in terms of relieving the compressional stress, while still maintaining a near-optimal C_{60}-C_{60} van der Waals bond length.

The next issue to consider is the domain width. LEED does not give information about positions within the surface unit cell, so that it is quite possible and even likely that the C_{60} molecules have rearranged themselves to relax from the $c(4\times4)$ structure. Such a relaxation would manifest itself in a progressive displacement from the hypothetical site indicated in Fig. 14, until the last molecule in such a displaced chain makes the jump up or down one row to start a new domain. Thus we speculate that the domain width is inherently limited by the importance of the bonding site for C_{60} on this substrate. This implies also that the largest separation indicated for this phase at the stripe boundaries is likely to be an overestimate; it should in any case be taken as an upper limit.

In the case of Al(111), the NND for all molecules in the metastable $(2\sqrt{3}\times2\sqrt{3})R30°$ C_{60} overlayer is 9.91 Å, identical to the shortest bond distance on Al(110). Hence, one explanation of why the (6×6) structure represents an energy minimum can be obtained by considering the ways in which a hexagonal overlayer can reconstruct in the direction perpendicular to the surface in order to increase this C_{60}-C_{60} separation.[77] Figure 15 is a comparison between three possible reconstructions: (a) alternate raised row, (b) zig-zag alternate raised rows, and (c) (6×6). Common to all three reconstructions is that the ratio of the number of short (9.91

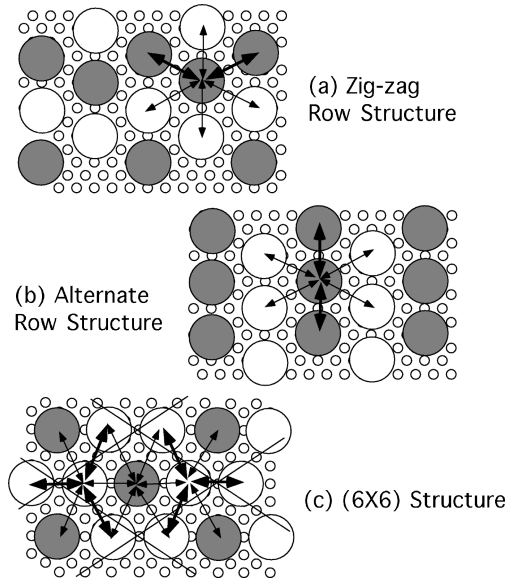

FIG. 15. Three possible vertical reconstructions of a horizontal two-dimensional hexagonal C_{60} lattice, occurring in order to increase the average C_{60}-C_{60} separation. The thick arrows indicate shorter bonds, and the thin arrows indicate longer, bulk-C_{60}-like bonds. The (6×6) structure is distinguished as requiring the least number of molecules to be displaced vertically, and for no nearest neighbors to be displaced. The ratio of long to short bonds in all three cases is 2:1.

Å) to long (≈10.09 Å based on STM measurements; see below) bond lengths is always 1:2; all other structures involving such vertical displacements yield a larger, and therefore energetically less favorable, ratio. The distinct feature of the (6×6) structure, however, is that it requires a vertical displacement of only 1/3 of the molecules, instead of 1/2, as for the other two structures. If displacement of the molecules away from the surface requires a net energy input in order to partially break the Al-Al bonds, the number of such displacements will tend to be minimized. This energy would clearly be smaller for the (6×6) structure than for any other reconstruction, and this structure would therefore represent an energy minimum. However, it is not at all clear that a net energy input is required for this reconstruction to occur, since STS shows that, in forming the (6×6) overlayer, C_{60} molecules are able to strengthen their bonding to Al specifically in the raised positions.[26] This must lead to an energy gain, partially or totally offseting the cost of breaking the Al-Al bonds. We therefore speculate that the primary reason that the (6×6) structure is favored over the alternative structures may be due to the fact that no adjacent molecules are displaced in such an overlayer. If the C_{60}-Al bond has polar character, as is the case for, e.g., Al covalently-bonded to carbon polymers[79–81] a dipole would be induced on each C_{60}-Al complex, energetically disfavoring structures where adjacent molecules are elevated. The apparent displacement of one third of the molecules by ≈1.9 Å obtained from STM (Ref. 26) suggests a bond distance of $(9.91+1.9)^{1/2}$ ≈10.09 Å, some 0.5% larger than the van der Waals NND for solid C_{60}, and this increase in equilibrium bond distance is consistent with the present proposition of repulsion between dipolar complexes.

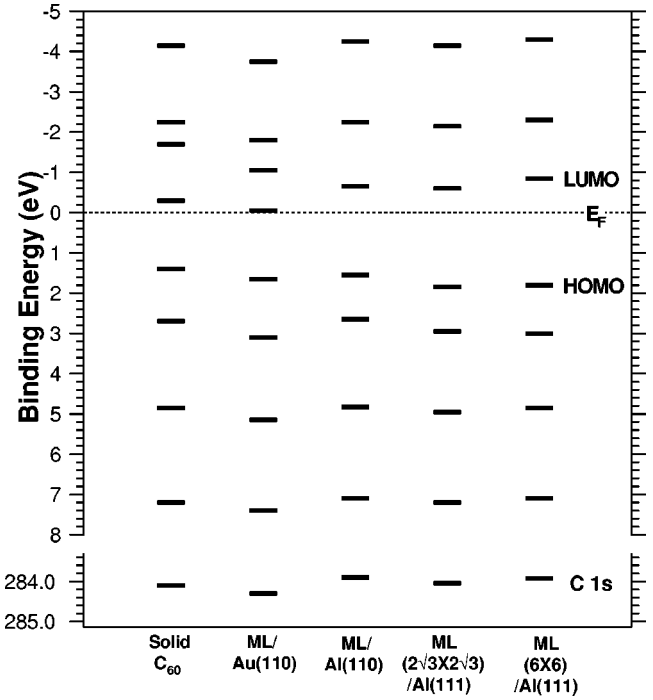

FIG. 16. The energy levels of the C_{60} monolayer systems and of solid C_{60}, from XAS and PES measurements. See the discussion in the text.

2. Electronic structure of the C_{60}-Al covalent bond

In Fig. 16 we summarize the energies of the occupied and unoccupied valence levels obtained from PES and XAS, for solid C_{60}, the three monolayer phases on Al, and 1 ML C_{60}/Au(110). For the monolayer systems, the position of E_F for the unoccupied valence band in the XAS spectra is taken to be equal to the C 1*s* binding energy.[82] In the case of multilayered C_{60}, the insulating nature of the film means that binding energies referenced to E_F of a metal substrate vary depending on film thickness and substrate work function.[47] Thus the alignment used in Fig. 16 is arbitrary for this case. However, in order to more clearly illustrate the effects of charge transfer, we align the σ-like solid C_{60} levels (near 5 and 7 eV binding energy) with those of (6×6)C_{60}/Al(111), for which the bonding is predominantly covalent. This is also justifiable because for the occupied states we find that for the valence levels below the HOMO-1, and for the C 1*s* level, the binding energies shift rigidly between these different systems. That the C 1*s* level shifts rigidly with the σ-like levels can be attributed to the uniform screening of a core hole,[52] which results in a similar charge distribution as in valence photoionization. Similar considerations apply for the levels seen in XAS above 286 eV. Charge transfer has been observed for C_{60}/Au(110) with both PES and HREELS,[18,16] and the shift seen in Fig. 16 between monolayers on Au(110) and on Al can perhaps be related to the charge state, so that the filling of the LUMO produces a downward shift in all other levels. We note that such a shift has recently been observed for the surface layer of graphite upon adsorption of K.[83] The situation here is clearly different from K on graphite, since, e.g., the DOS at the LUMO is significantly larger than for the π-derived states immediately above E_F in graphite, and within a simple rigid band model smaller shifts would there-

fore be expected here. C 1*s* binding energies for[60] K_3C_{60} and a conducting superfulleride[61] (where the t_{1g} level is partly filled and $\approx$11 electrons are transfered to the fullerene) are both close to 284.6 eV, implying that the final-state screening effects are also important.

When atoms and molecules are adsorbed on simple metal surfaces, the valence levels shift to lower energy (i.e., higher binding energy for the occupied states) as the strength of the adsorbate-substrate bonding interaction increases.[84–86] The size of this energy shift should be related to the magnitude of the interaction matrix element, and will therefore be greater for the more delocalized π-like frontier levels. This is clearly the case here for C_{60} monolayers on Al, and is reminiscent of the behavior of benzene on a series of metal surfaces.[87] However such a model involving interaction of the fullerene molecular orbitals with delocalized bands may not be sufficient for a correct description of more localized bonding behavior in the present case. We noted above in Secs. III B 1 and III B 3 that the structure above the ionization potential in XAS, and degeneracy lifting observed in the HOMO, reflect changes in the physical structure of the molecules. If the C atoms become more sp^3-bonded as C_{60} bonds covalently to Al atoms, we may expect this character to be mixed in with the wave functions of the mainly π-derived HOMO, HOMO-1, and LUMO. In the case of photopolymerized C_{60},[64] this has the effect of increasing the LUMO energy, and this is probably the reason for the increase in energy of the LUMO resonance with interaction strength observed here, suggesting that this more local description is the most appropriate. The presence of C_{60}-derived DOS extending to E_F in the PES data for all three monolayer systems on Al implies that the HOMO-derived states may become partly unoccupied. Since the highest lying parts of the HOMO resonance are likely to be the most C_{60}-Al antibonding, this will increase the strength of the bond.

3. Comparison of Al(110) and Al(111)

It may at first glance seem surprising that the interaction with C_{60} is weaker for Al(110) than Al(111). Al(110) is the more open surface, and generally considered to be the more reactive. However, it has recently been shown using photoelectron diffraction[88] and STM/STS (Ref. 27) that C_{60} is adsorbed on Al(111) with a six-membered ring towards the surface. Figures 2 and 15 show a possible adsorption geometry in which six C atoms are able to some extent to coordinate to six Al atoms. Since there are three double bonds around each hexagon, we speculate that these can be broken (or modified) and sp^3 bonds can be thereby formed with the Al atoms in a manner similar to what is calculated to occur at Al-polymer interfaces.[79–81] In the case of Al(110), however, no such high-symmetry coordinated site exists, due to the rectangular structure of the surface.

We find that C_{60} monolayers are desorbed from both surfaces at temperatures close to 730 K, and this may appear to contradict our results showing different interaction strengths on the two surfaces. However, the evidence presented here from spectroscopy data relate to the strength of the perturbation of the electronic and physical structure of the molecule due to the substrate-adsorbate bond, and this cannot generally be expected to correspond to the overall bond strength. If one thinks again in terms of energy balance, small differences in the charge state, not observable here, could result in a new term that could increase the total bond strength. In addition, the reversal of the Al(111) surface reconstruction upon desorption of C_{60} would result in an additional energy input in the desorption process, effectively lowering the barrier for desorption on Al(111). LEED shows that the surface returns to the (1×1) symmetry upon desorption of a (6×6) overlayer, giving credence to this hypothesis.

The C_{60}-Al interaction is therefore an interesting and somewhat special case. First of all, Al is a simple metal with free electron character and a work function that is lower than those of low-index surfaces of Au, Ag and Cu.[75] One model predicts that charge transfer should increase with decreasing work function.[89] However, Al adsorbed on polymer surfaces is found to bond covalently with the C atoms of the chains,[79–81,90] changing the structure of the molecule as C atoms form polar-covalent sp^3-like bonds with Al atoms; similar calculations suggest a comparable pattern for bonding between C_{60} and isolated Al atoms,[91] and for Al and C in general.[92] We also note that the cohesive energy of Al lies between that of alkali metals (for which, e.g., for C_{60} deposited on K multilayers, the K moves extensively to engulf the fullerenes[61]) and all of the other metals discussed in association with Table I. The present work makes clear the possibilities and pitfalls in the production of tailored C_{60}-Al architectures, in that, e.g., transport properties[93] could be strongly dependent on the interface structures adopted, as well as the manner in which the interface is constructed.[94]

IV. CONCLUSIONS

We have characterized two new ordered C_{60} monolayer structures. In addition to the (6×6) structure formed at 620 K on Al(111),[25,26] we find that C_{60} forms a metastable phase when adsorbed at room temperature consisting of a $(2\sqrt{3}\times2\sqrt{3})R30°$ overlayer. On Al(110), a pseudo-$c(4\times4)$ ordered monolayer can be formed at 620 K. However, no new, reconstruction-induced peak is observed in the Al 2*p* PES spectrum as was observed for the (6×6) phase on Al(111). Superstructure occuring in the $c(4\times4)$ overlayer can instead be understood in terms of relieving of the inherent intralayer compression, causing relaxation parallel to the surface and resulting in a series of stripelike domains. The formation of the (6×6) structure, on the other hand, can be partly understood in terms of repulsion between surface dipoles adding to the relatively small compression energy, in addition to an bonding geometry particularly favorable for a strong covalent bond. No evidence for charge transfer is observed on either surface at 300 K, and the interaction with the substrate is predominantly covalent for all phases of C_{60}/Al studied here. Measurements of the work function for these and other C_{60} monolayer films are not well described within a simple dipole model, suggesting that the fundamental dielectric response of the metal-chemisorbed C_{60} layer is defining the results obtained.

Symmetry-breaking-induced splitting is observed in the valence PES data in all three systems, and the broadening of the spectra becomes stronger in the series pseudo-$c(4\times4)$ C_{60}/Al(110), $(2\sqrt{3}\times2\sqrt{3})R30°$/Al(111), (6×6)/Al(111). C 1*s* XAS and shakeup show that the perturbation on the elec-

tronic and geometric structure of the fullerene molecules due to the bonding interaction with the surface increases with the same trend. However, the desorption temperature of monolayers on both substrates are approximately 730 K, and the difference between information about the relative bond strengths from these varying methods may be due to extra terms in the energy balance governing the desorption process, e.g., resulting from small differences in charge state and the reversal of the Al(111) reconstruction.

We suggest that the bonding of C_{60} to surfaces can be divided into four categories, three of which correspond to previously studied cases: weak, predominantly van der Waals; intermediate, predominantly ionic, where charge is observed in the LUMO and $T_{desorb} = 700$-850 K; and strong bonding where $T_{desorb} > 1000$ K or C_{60} decomposes, and the bonding has mainly covalent character. In terms of mobility on the surface and desorption temperature, the C_{60}-Al systems studied here share many characteristics of the group of metals including Au, Ag, and Cu, which bond ionically to C_{60}. The evidence for covalent bonding therefore puts Al in a new category of intermediate covalent bonding as far as its interaction with C_{60} is concerned.

ACKNOWLEDGMENTS

We acknowledge useful and stimulating discussions with J. N. Andersen, S. M. Gray, A. Santaniello, R. Fasel, S. Modesti, E. Tosatti, E. L. Bullock, L. Patthey, and P. Rudolf, and the able technical assistance of J.-O. Forsell and L. Bolkegård. This work was funded in part by the Swedish National Science Research Council (NFR) and the Swedish Materials Research Consortium on Clusters and Ultrafine Particles, which is funded by NFR and NUTEK, the Swedish National Board for Industrial and Technical Development.

*Present address: Swedish Transmission Research Institute, Box 707, S-771 80 Ludvika, Sweden.

† Electronic address: paul@fysik.uu.se

[1] A. J. Maxwell, P. A. Brühwiler, A. Nilsson, N. Mårtensson, and P. Rudolf, Phys. Rev. B **49**, 10 717 (1994).

[2] J. K. Gimzewski, S. Modesti, and R. R. Schlittler, Phys. Rev. Lett. **72**, 1036 (1994).

[3] B. Reihl, in *Science and Technology of Fullerene Materials*, edited by P. Bernier, T. W. Ebbesen, D. S. Bethune, R. M. Metzger, L. Y. Chiang, and J. W. Mintmire, MRS Symposia Proceedings No. 359 (Materials Research Society, Pittsburgh, 1995), p. 375.

[4] M. Pedio, M. L. Grilli, C. Ottaviani, M. Capozi, C. Quaresima, P. Perfetti, P. A. Thiry, R. Caudano, and P. Rudolf, J. Electron Spectrosc. Relat. Phenom. **76**, 405 (1995).

[5] P. A. Gravil, Ph. Lambin, G. Gensterblum, L. Henrad, P. Senet, and A. A. Lucas, Surf. Sci. **329**, 199 (1995).

[6] M. R. C. Hunt and R. E. Palmer, Surf. Rev. Lett. **3**, 937 (1996).

[7] P. A. Brühwiler, A. J. Maxwell, P. Baltzer, S. Andersson, D. Arvanitis, L. Karlsson, and N. Mårtensson, Chem. Phys. Lett. **279**, 92 (1997).

[8] A. V. Hamza and M. Balooch, Chem. Phys. Lett. **201**, 404 (1993).

[9] ''Rapidly'' here is taken to mean easily measurable on the monolayer scale, i.e., relevant for the present study.

[10] G. Gensterblum, K. Hevesi, B.-Y. Han, L.-M. Yu, J.-J. Pireaux, P. A. Thiry, R. Caudano, A.-A. Lucas, D. Bernaerts, S. Amelinckx, G. Van Tendeloo, G. Bendele, T. Buslaps, R. L. Johnson, M. Foss, R. Feidenhans'l, and G. Le Lay, Phys. Rev. B **50**, 11 981 (1994).

[11] J.-M. Themlin, S. Bouzidi, F. Coletti, J.-M. Debever, G. Gensterblum, L.-M. Yu, J.-J. Pireaux, and P. A. Thiry, Phys. Rev. B **46**, 15 602 (1992).

[12] G. Gensterblum, L. M. Yu, J.-J. Pireaux, P. A. Thiry, and R. Caudano, Appl. Phys. A: Solids Surf. **56**, 175 (1993).

[13] D. Schwartz, W. Allers, G. Gensterblum, J. Pireaux, and R. Wiesendanger, Phys. Rev. B **52**, 5967 (1995).

[14] E. I. Altman and R. J. Colton, Surf. Sci. **295**, 13 (1993).

[15] S. Modesti, R. R. Schlittler, and J. K. Gimzewski, Surf. Sci. **331-333**, 1129 (1995).

[16] S. Modesti, S. Cerasari, and P. Rudolf, Phys. Rev. Lett. **71**, 2469 (1993).

[17] M. R. C. Hunt, S. Modesti, P. Rudolf, and R. E. Palmer, Phys. Rev. B **51**, 10 039 (1995).

[18] P. Rudolf (private communication).

[19] G. K. Wertheim and D. N. E. Buchanan, Phys. Rev. B **50**, 11 070 (1994).

[20] K.-D. Tsuei, J.-Y. Yuh, C.-T. Tzeng, R.-Y. Chu, S.-C. Chung, and K.-L. Tsang, Phys. Rev. B **56**, 15 412 (1997).

[21] S. J. Chase, W. S. Bacsa, M. G. Mitch, L. J. Pilione, and J. S. Lannin, Phys. Rev. B **46**, 7873 (1992).

[22] J. E. Rowe, P. Rudolf, L. H. Tjeng, R. A. Malic, G. Meigs, C. T. Chen, J. Chen, and E. W. Plummer, Int. J. Mod. Phys. B **6**, 3909 (1992).

[23] K.-D. Tsuei and P. D. Johnson, Solid State Commun. **101**, 337 (1997).

[24] R. Lüthi, E. Meyer, H. Haefke, L. Howald, W. Gutmannsbauer, and H.-J. Güntherodt, Science **266**, 1979 (1994).

[25] A. J. Maxwell, P. A. Brühwiler, S. Andersson, D. Arvanitis, B. Hernnäs, O. Karis, D. C. Mancini, N. Mårtensson, S. M. Gray, M. K.-J. Johansson, and L. S. O. Johansson, Phys. Rev. B **52**, R5546 (1995).

[26] M. K.-J. Johansson, A. J. Maxwell, S. M. Gray, P. A. Brühwiler, D. C. Mancini, L. S. O. Johansson, and N. Mårtensson, Phys. Rev. B **54**, 13 472 (1996).

[27] M. K.-J. Johansson, A. J. Maxwell, S. M. Gray, P. A. Brühwiler, and L. S. O. Johansson, Surf. Sci. **397**, 314 (1998).

[28] T. David, J. K. Gimzewski, D. Purdie, B. Reihl, and R. R. Schlittler, Phys. Rev. B **50**, 5810 (1994).

[29] J. K. Gimzewski, S. Modesti, T. David, and R. R. Schlittler, J. Vac. Sci. Technol. B **12**, 1942 (1994).

[30] P. W. Murray, M. Ø Pedersen, E. Laegsgaard, I. Stensgaard, and F. Besenbacher, Phys. Rev. B **55**, 9360 (1997).

[31] T. Hashizume and T. Sakurai, J. Vac. Sci. Technol. B **12**, 1992 (1994).

[32] D. Klyachko and D. M. Chen, Phys. Rev. Lett. **75**, 3693 (1995).

[33] S. Henke, M. Philipp, B. Rauschenbach, and B. Stritzker, in *Physics and Chemistry of Fullerenes and Derivatives*, edited by H. Kuzmany, J. Fink, M. Mehring, and S. Roth (World Scientific, Singapore, 1995), p. 81.

[34] D. M. Chen, H. Xu, W. N. Creager, and P. Burnett, J. Vac. Sci. Technol. B **12**, 1910 (1994).
[35] H. Xu, D. M. Chen, and W. N. Creager, Phys. Rev. B **50**, 8454 (1994).
[36] C. Cepek, A. Goldoni, and S. Modesti, Phys. Rev. B **53**, 7466 (1996).
[37] P. Rudolf, in *Fullerenes and Fullerene Nanostructures*, edited by H. Kuzmany, J. Fink, M. Mehring, and S. Roth (World Scientific, Singapore, 1996), p. 263.
[38] T. Sakurai, X.-D. Wang, Q. K. Xue, Y. Hasegawa, T. Hashizume, and H. Shinohara, Prog. Surf. Sci. **51**, 263 (1996).
[39] E. I. Altman and R. J. Colton, in *Recent Advances in the Chemistry and Physics of Fullerenes and Related Materials*, edited by K. M. Kadish and R. S. Ruoff (The Electrochemical Society, Inc., Pennington, NJ, 1994), p. 431.
[40] E. I. Altman and R. J. Colton, Surf. Sci. **279**, 49 (1992).
[41] J. K. Gimzewski, S. Modesti, and R. R. Schlittler, Chem. Phys. Lett. **213**, 401 (1993).
[42] T. Yamaguchi, J. Vac. Sci. Technol. B **12**, 1932 (1994).
[43] D. Chen and D. Sarid, Surf. Sci. **329**, 206 (1995).
[44] D. Chen, J. Chen, and D. Sarid, Phys. Rev. B **50**, 10 905 (1994).
[45] Y.-R. Ma, P. Moriarty, and P. H. Beton, Phys. Rev. Lett. **78**, 2588 (1997).
[46] J. N. Andersen, O. Björneholm, A. Sandell, R. Nyholm, J.-O. Forsell, L. Thånell, A. Nilsson, and N. Mårtensson, Synchr. Rad. News **4** (4), 15 (1991).
[47] A. J. Maxwell, P. A. Brühwiler, D. Arvanitis, J. Hasselström, and N. Mårtensson, Chem. Phys. Lett. **260**, 71 (1996).
[48] P. A. Heiney, J. Phys. Chem. Solids **53**, 1333 (1992).
[49] R. Nyholm, J. N. Andersen, J. F. van Acker, and M. Qvarford, Phys. Rev. B **44**, 10 987 (1991).
[50] S. Tanuma, C. J. Powell, and D. R. Penn, Surf. Interface Anal. **17**, 911 (1991).
[51] We use PES to denote that we excite the core levels to relatively low kinetic energies.
[52] E. Rotenberg, C. E. Enkvist, P. A. Brühwiler, A. J. Maxwell, and N. Mårtensson, Phys. Rev. B **54**, R5279 (1996).
[53] W. E. Pickett, in *Solid State Physics, Fullerenes*, edited by H. Ehrenreich and F. Spaepen (Academic, San Diego, 1994), p. 231.
[54] T. R. Ohno, Y. Chen, S. E. Harvey, G. H. Kroll, J. H. Weaver, R. E. Haufler, and R. E. Smalley, Phys. Rev. B **44**, 13 747 (1991).
[55] M. W. Ruckman, B. Xia, and S. L. Qiu, Phys. Rev. B **48**, 15 457 (1993).
[56] G. K. Wertheim and D. N. E. Buchanan, Solid State Commun. **88**, 97 (1993).
[57] L. Q. Jiang and B. E. Koel, Chem. Phys. Lett. **223**, 69 (1994).
[58] R. Fasel, R. G. Agostino, P. Aebi, and L. Schlapbach, (unpublished).
[59] D. Purdie, H. Bernhoff, and B. Reihl, Surf. Sci. **364**, 279 (1996).
[60] P. A. Brühwiler, A. J. Maxwell, A. Nilsson, N. Mårtensson, and O. Gunnarsson, Phys. Rev. B **48**, 18 296 (1993).
[61] A. J. Maxwell, P. A. Brühwiler, S. Andersson, N. Mårtensson, and P. Rudolf, Chem. Phys. Lett. **247**, 257 (1995).
[62] C. Enkvist, S. Lunell, B. Sjögren, S. Svensson, P. A. Brühwiler, A. Nilsson, A. J. Maxwell, and N. Mårtensson, Phys. Rev. B **48**, 14 629 (1993).
[63] P. Rudolf, P. A. Brühwiler, A. J. Maxwell, S. Andersson, and N. Mårtensson (unpublished).
[64] B. S. Itchkawitz, J. P. Long, T. Schedel-Niedrig, M. N. Kabler, A. M. Bradshaw, R. Schlögl, and W. R. Hunt, Chem. Phys. Lett. **243**, 211 (1995).
[65] J. Stöhr, *NEXAFS Spectroscopy* (Springer-Verlag, Berlin, 1992).
[66] A. J. Maxwell, P. A. Brühwiler, D. Arvanitis, J. Hasselström, and N. Mårtensson, Phys. Rev. Lett. **79**, 1567 (1997).
[67] When dicussing the variations in the interaction strength between C_{60} and the substrate for the different phases found on Al(111) and Al(110), by the use of the term interaction strength we refer to the perturbation on the electronic and geometric structure of the C_{60} molecules resulting from the bonding interaction with the substrate, as opposed to the overall bond strength judged from the desorption temperatures. We discuss the relationship between the interaction strength and the desorption temperature in Sec. III C 3.
[68] M. Scheffler and A. M. Bradshaw, in *Adsorption at Solid Surfaces*, edited by D.A. King and D.P. Woodruff (Elsevier, Amsterdam, 1983), p. 165.
[69] Y. C. Chen, J. E. Cunningham, and C. P. Flynn, Phys. Rev. B **30**, 7317 (1984).
[70] G. Herzberg, *Atomic Spectra and Atomic Structure* (Dover, New York, 1944), p. 219.
[71] D. L. Lichtenberger, M. E. Jatcko, K. W. Nebesny, C. D. Ray, D. R. Huffman, and L. D. Lamb, in *Clusters and Cluster-Assembled Materials*, edited by D. Green, K. Sieradzki, and L. J. Gibson, MRS Symposia Proceedings No. 206 (Materials Research Society, Pittsburgh, 1991), p. 673.
[72] O. Gunnarsson, H. Handschuh, P. S. Bechthold, B. Kessler, G. Ganteför, and W. Eberhardt, Phys. Rev. Lett. **74**, 1875 (1995).
[73] J. K. Grepstad, P. O. Gartland, and B. J. Slagsvold, Surf. Sci. **57**, 348 (1976).
[74] G. A. Benesh and D. Gebreselasie, Phys. Rev. B **54**, 5940 (1996).
[75] *CRC Handbook of Chemistry and Physics*, edited by R. C. Weast (CRC, Boca Raton, Florida, 1994).
[76] E. Bertel, G. Rosina, and F. P. Netzer, Surf. Sci. **172**, L515 (1986).
[77] This separation is not much smaller than that of the low-temperature C_{60} solid, as noted in Sec. III A 1. However, the unique molecular arrangement necessary to achieve this compression from the room-temperature separation is likely inhibited by the optimization of the bond to the substrate. Thus, we assume that there is a significant compressional stress in the overlayers for the unrelaxed structures.
[78] We use the term ''position'' defined relative to the overlayer, in order not to confuse this with the common term ''site,'' which is defined relative to the substrate. Thus the adsorption site shown in Fig. 14 is arbitrary. The fact that commensurate structures are at all observed, however, indicates that one adsorption site is preferred, and the choice of site does not affect our model.
[79] A. Calderone, R. Lazzaroni, and J. L. Brédas, Phys. Rev. B **49**, 14 418 (1994).
[80] M. Boman, S. Stafström, and J. L. Brédas, J. Chem. Phys. **97**, 9144 (1992).
[81] C. Fredriksson and J. L. Brédas, J. Chem. Phys. **98**, 4253 (1993).
[82] A. Nilsson, O. Björneholm, E. O. F. Zdansky, H. Tillborg, N. Mårtensson, J. N. Andersen, and R. Nyholm, Chem. Phys. Lett. **197**, 12 (1992).
[83] P. Bennich, C. Puglia, P. A. Brühwiler, A. Nilsson, A. J. Maxwell, A. Sandell, N. Mårtensson, and P. Rudolf (unpublished).
[84] J. K. Nørskov, Rep. Prog. Phys. **53**, 1253 (1990).
[85] N. D. Lang and A. R. Williams, Phys. Rev. B **18**, 616 (1978).

[86] B. Hammer, Y. Morikawa, and J. K. Nørskov, Phys. Rev. Lett. **76**, 2141 (1996).
[87] F. P. Netzer, Langmuir **7**, 2544 (1991).
[88] R. Fasel, P. Aebi, R. G. Agostino, D. Naumovic, J. Osterwalder, A. Santaniello, and L. Schlapbach, Phys. Rev. Lett. **76**, 4733 (1996).
[89] E. Burstein, S. C. Erwin, M. Y. Jiang, and R. P. Messmer, Phys. Scr. **T41**, 1 (1992).
[90] P. Dannetun, M. Boman, S. Stafström, W. R. Salaneck, R. Lazzaroni, C. Fredriksson, J. L. Brédas, R. Zamboni, andC. Taliani, J. Chem. Phys. **99**, 664 (1993).
[91] S. Stafström (unpublished).
[92] A. P. Seitsonen, K. Laasonen, R. M. Nieminen, and M. L. Klein, J. Chem. Phys. **103**, 8075 (1995).
[93] A. F. Hebard, C. B. Eom, Y. Iwasa, K. B. Lyons, G. A. Thomas, D. H. Rapkine, R. M. Fleming, R. C. Haddon, J. M. Phillips, J. H. Marshall, and R. H. Eick, Phys. Rev. B **50**, 17 740 (1994).
[94] D. W. Owens, C. M. Aldao, D. M. Poirier, and J. H. Weaver, Phys. Rev. B **51**, 17 068 (1995).